Acta Neurochirurgica
https://doi.org/10.1007/s00701-019-04152-4

ORIGINAL ARTICLE - NEUROSURGICAL ANATOMY

Quantitative anatomical comparison of transnasal and transcranial approaches to the clivus

Edoardo Agosti[1] · Giorgio Saraceno[1] · Jimmy Qiu[2] · Barbara Buffoli[3] · Marco Ferrari[4] · Elena Raffetti[5] · Francesco Belotti[1] · Marco Ravanelli[6] · Davide Mattavelli[4] · Alberto Schreiber[4] · Lena Hirtler[7] · Luigi F. Rodella[3] · Roberto Maroldi[6] · Piero Nicolai[4] · Fred Gentili[8] · Walter Kucharczyk[9] · Marco M. Fontanella[1] · Francesco Doglietto[1]

Received: 7 October 2019 / Accepted: 18 November 2019

Abstract

Background and objective The clivus was defined as "no man's land" in the early 1990s, but since then, multiple approaches have been described to access it. This study is aimed at quantitatively comparing endoscopic transnasal and microsurgical transcranial approaches to the clivus in a preclinical setting, using a recently developed research method.

Methods Multiple approaches were performed in 5 head and neck specimens that underwent high-resolution computed tomography (CT): endoscopic transnasal (transclival, with hypophysiopexy and with far-medial extension), microsurgical anterolateral (supra-orbital, mini-pterional, pterional, pterional transzygomatic, fronto-temporal-orbito-zygomatic), lateral (subtemporal and subtemporal transzygomatic), and posterolateral (retrosigmoid, far-lateral, retrolabyrinthine, translabyrinthine, and transcochlear). An optic neuronavigation system and dedicated software were used to quantify the working volume of each approach and calculate the exposure of different clival regions. Mixed linear models with random intersections were used for statistical analyses.

Results Endoscopic transnasal approaches showed higher working volume and larger exposure compared with microsurgical transcranial approaches. Increased exposure of the upper clivus was achieved by the transnasal endoscopic transclival approach with intradural hypophysiopexy. Anterolateral microsurgical transcranial approaches provided a direct route to the anterior surface of the posterior clinoid process. The transnasal endoscopic approach with far-medial extension ensured a statistically larger exposure of jugular tubercles as compared with other approaches. Presigmoid approaches provided a relatively limited exposure of the ipsilateral clivus, which increased in proportion to their invasiveness.

Conclusions This is the first anatomical study that quantitatively compares in a holistic way exposure and working volumes offered by the most used modern approaches to the clivus.

Keywords Clivus · Comparative study · Endoscopy · Microsurgery · Quantitative study · Skull base surgery

This article is part of Topical Collection on *Neurosurgical Anatomy*

Electronic supplementary material The online version of this article https://doi.org/10.1007/s00701-019-04152-4) contains supplementary material, which is available to authorized users.

✉ Francesco Doglietto
francesco.doglietto@unibs.it

[1] Neurosurgery, Department of Medical and Surgical Specialties, Radiological Sciences and Public Health, University of Brescia, Largo Spedali Civili, 1, 25123 Brescia, Italy

[2] TECHNA Institute, University Health Network, Toronto, Ontario, Canada

[3] Section of Anatomy and Physiopathology, Department of Clinical and Experimental Sciences, University of Brescia, Brescia, Italy

[4] Otorhinolaryngology, Department of Medical and Surgical Specialties, Radiological Sciences and Public Health, University of Brescia, Brescia, Italy

[5] Department of Public Health Sciences, Karolinska Institute, Stockholm, Sweden

[6] Radiology, Department of Medical and Surgical Specialties, Radiological Sciences and Public Health, University of Brescia, Brescia, Italy

[7] Division of Anatomy, Center for Anatomy and Cell Biology, Medical University of Vienna, Vienna, Austria

[8] Department of Neurosurgery, Toronto Western Hospital, University of Toronto, Toronto, Ontario, Canada

[9] Department of Medical Imaging, University of Toronto, Toronto, Canada

Published online: 02 December 2019

Introduction

In the early 1990s, Samii and Knosp defined the clivus "no man's land" due to the difficulty of accessing it [37]. During the last three decades, different approaches to this complex skull base region have been described. These include microsurgical transcranial approaches (MTCAs) [22–25] and, more recently, endoscopic transnasal transclival approaches (ETCAs) [22–25].

As opinions are still conflicting on what might be the best approach/es to reach the different portions of the clivus for different pathologies [8, 9, 28, 31], following the IDEAL recommendations for surgical research [6, 13, 30], this preclinical study was conceived, as an evolution of previous ones [10, 11], with the aim of providing a systematic and objective comparison of all the most used approaches to the clivus. A novel research method, based on neuronavigation, was implemented, with specific software that quantifies the working volume and the area of exposure provided by a surgical approach [2, 10, 11, 14, 15, 20, 35, 39].

Materials and methods

The study was conducted in accordance with institutional ethical committee guidelines.

Specimens

A total of 5 specimens (10 sides) were dissected. Intracranial arteries were injected via the common carotid and vertebral arteries with a silicone rubber composed of a base and a catalyst (Xiameter® RTV rubber base and curing agent, Dow Corning®, Midland, MI, USA) colored with red-stained silicone Pintasol® (Mixol® Red E-L3mix, Kirchheim unter Teck, Germany).

CT scans

Each specimen underwent a CT scan using a multidetector 128-slice scanner (Somatom Definition Flash®, Siemens, Forchheim, Germany). The acquisition was conducted from the vertex to the fifth cervical vertebra. CT parameters included tube tension 120 kV, tube current 280 mAs (with dose modulation), and collimation 0.6 mm. Images were reconstructed at 1 mm (increment 0.7 mm) with a soft tissue kernel. Subsequently, each specimen CT scan was rectified manually using the CT machinery workstation by rotating CT scans on a coronal plane to maintain the two internal acoustic canals (IACs), glossopharyngeal canals, and hypoglossal canals on the same axial images, respectively. CT scan files were recorded on a CD in Digital Imaging and Communications in Medicine (DICOM) format.

Surgical approaches

All dissections were performed in the Anatomy Laboratory of the University of Brescia.

Standard neurosurgical instrument sets were used. Endoscopic surgical instruments were part of the Storz® endoscopic pituitary and skull base surgery set (Karl Storz®, Tüttlingen, Germany). The surgical microscope Leica® M320 (Leica Microsystems Srl, Buccinasco, Italy) and 2D HD head-camera (Karl Storz®, Tüttlingen, Germany) with 0° optics (Karl Storz®) were respectively used for microsurgical and endoscopic visualization. High-speed drills and craniotome (Anspach®, High Wycombe, UK) were used.

The following ETCAs were performed and quantified (Fig. 1):

1. *Endoscopic transnasal transclival approach* (*ETCA*), as described by De Notaris et al. [9]. A posteroinferior septectomy, dissection of the nasopharyngeal posterior wall, and drilling of the sphenoid floor were performed. The clivectomy was completed, respecting the dura and considering the following limits: the paraclival internal carotid artery (ICA) and hypoglossal nerves laterally, sellar floor superiorly, and foramen magnum inferiorly.
2. *ETCA with intradural hypophysiopexy approach* (*ETCAH*), according to Kassam et al. [26]. The sellar floor and tuberculum sellae were drilled, the sellar periosteum opened, and the diaphragma sellae cut. Both inferior hypophyseal arteries were cut; the entire pituitary gland was displaced in the suprasellar cistern. Finally, the dorsum sellae was removed.
3. *ETCA with far-medial extension* (*ETCAFM*), according to Beltrán-Giner et al. [4]. The neurovascular pterygoid structures were exposed, Eustachian tube transposed, and the anteromedial portion of the ipsilateral occipital condyle was drilled. The hypoglossal canal was opened and the nerve exposed. The medial portion of the jugular tuberculum was drilled and the lower cranial nerves identified.

The following anterolateral MTCAs were investigated (Supplementary Fig. 1):

1. *Supraorbital approach* (*SO*), as described by Perneczky [34]. After skin incision, a fronto-basal burr hole was placed just posterior to the anterior portion of the temporal line. The craniotomy was extended from the keyhole to

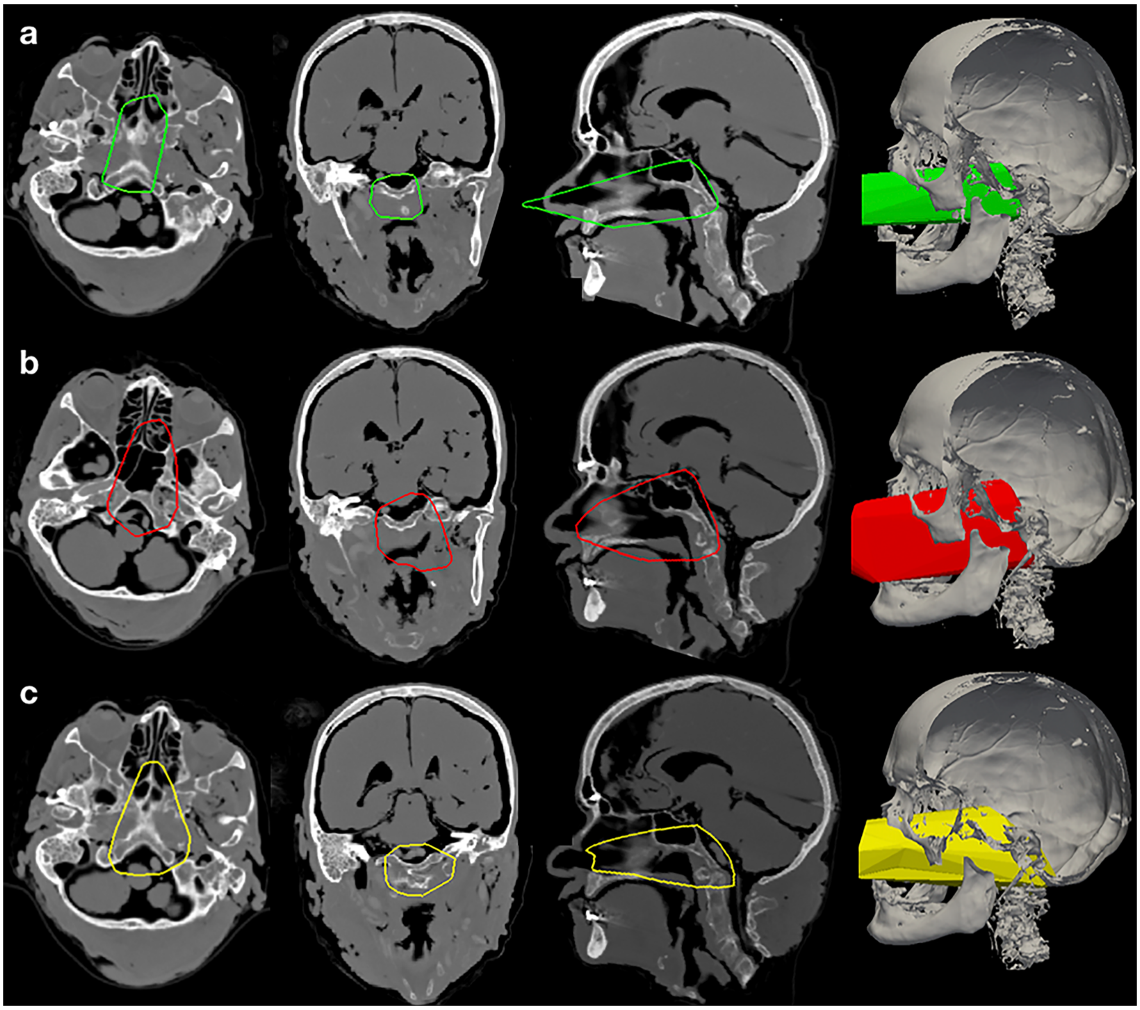

Fig. 1 Quantified crossing ETCAs to the clivus. Exemplificative screenshots from ApproachViewer (part of GTx-Eyes II – UHN – University of Toronto) in axial, coronal, and sagittal planes and 3-dimensional view of endoscopic transnasal approaches. **a** Transnasal endoscopic transclival approach. **b** ETCA with intradural hypophysiopexy. **c** ETCA with far-medial extension

the medial edge of the supraorbital rim. The frontal dura was incised along the roof of the orbit.

2. *Mini-pterional approach* (*MPT*), according to Figueiredo et al. [16]. An interfascial dissection was performed. The craniotomy was extended along the superior temporal line and curved downward to include the pterion and anteriorly up to the keyhole.
3. *Pterional approach* (*PT*), according to Yasargil [45]. A fronto-temporo-sphenoidal osteotomy was performed. Then, the lateral wall of the orbit and the lesser wing of the sphenoid bone were partially drilled to avoid any bony obstruction. Once the dura was incised, the Sylvian fissure was widely opened.
4. *Pterional transzygomatic approach* (*PTTZ*), as described by Campero et al. [5]. Starting from the pterional approach, the zygomatic arch was exposed and cut posteriorly, near the temporomandibular joint, and anteriorly just behind the zygomatic bone. The bone segment was reflected inferiorly with the masseter muscle.
5. *Fronto-temporal-orbito-zygomatic approach* (*FTOZ*), according to Van Furth et al. [42]. The craniotomy was performed in two steps, with the fronto-temporal craniotomy followed by the orbito-zygomatic one.

The following lateral MTCAs were performed and quantified (Supplementary Fig. 2):

1. *Subtemporal approach* (*ST*), as described by Dolenc [12]. A craniotomy with a 2.5-cm base parallel to the zygomatic arch and 2 cm high was performed. The temporal dura was opened and the temporal lobe was retracted superomedially for 1 cm in a standardized manner. The dura was detached from the skull base bone, cutting the middle meningeal artery at foramen spinosum, and the dissection proceeded extradurally.
2. *Subtemporal transzygomatic approach* (*STTZ*), according to Ustun et al. [41]. Starting from the subtemporal approach, the zygomatic arch was cut posteriorly near the

temporomandibular joint and anteriorly just behind the zygomatic bone and then removed.

The following posterolateral MTCAs were investigated (Fig. 2):

1. *Presigmoid retrolabyrinthine infratentorial approach* (*RL*), as described by Wanibuchi et al. [44]. A retroauricular C-shape incision was made. An open mastoidectomy was performed and the sigmoid and superior petrosal sinuses were exposed. Lateral, posterior, and superior semicircular canals were identified and preserved. The dural triangle bounded by the sigmoid sinus posteriorly, the labyrinth anteriorly, and superior petrosal sinus superiorly was incised.
2. *Presigmoid translabyrinthine infratentorial approach* (*TL*), according to Wanibuchi et al. [44]. After performing the RL, the labyrinth was drilled up to the internal auditory canal (IAC), which was subsequently opened. After completing the drilling, the dura deep to the labyrinth was uncovered and lanced in a T-shaped fashion.
3. *Presigmoid transcochlear infratentorial approach* (*TC*), in accordance with Wanibuchi et al. [44]. After performing the TL, the facial nerve was skeletonized from its entrance into the IAC to the stylomastoid foramen, and posterior rerouting of the facial nerve was performed. The cochlea was drilled starting from the basal turn to middle and apical turns, reaching the petrous ICA.
4. *Retrosigmoid approach* (*RS*), as described by Vender [43]. The sigmoid sinus was identified along the line connecting the zygomatic arch and the inion. A curved vertical incision was made two fingers behind the insertion of the pinna. The burr hole was placed on the asterion and a suboccipital craniectomy was performed. The dural incision was performed parallel to the sigmoid sinus.
5. *Far-lateral approach* (*FL*), according to Rhoton [36]. A hockey stick incision along the posterior midline of the neck was performed, approximately down to the level of C4. The V3 segment of the vertebral artery was exposed and a suboccipital craniectomy with ipsilateral C1 hemilaminectomy performed. The ipsilateral occipital condyle was drilled, performing the transcondylar variant of this approach. Finally, the RS dural incision was extended inferiorly to the cranial margin of C2.

Care was taken to ensure that all approaches were performed in a modular way, i.e., from the less invasive to the more extensive ones, to avoid any loss of information. Specifically, among ETCAs, ETCA was always performed first and randomly followed by ETCAH or ETCAFM. Anterolateral MTCAs were performed with this sequence: SO, MTP, PT, PTTZ, and FTOZ and then EAC. ST was followed by STTZ. Concerning posterolateral MTCAs, RS was always performed first and followed by FL and presigmoid approaches. Presigmoid approaches were performed by progressive invasiveness: RL, TL, and TC.

Surgical corridor quantification

After each approach was reproduced on the specimen, each surgical corridor was quantified with an optical neuronavigation system (Polaris Vicra®; NDI, Waterloo, Ontario, Canada) [11] coupled with dedicated software (ApproachViewer, part of GTx-Eyes II – UHN; University of Toronto, Toronto, Ontario, Canada) [7]. A neuronavigation error of less than 1 mm was considered acceptable for quantification.

Regarding the ETCAs (ETCA, ETCAH, and ETCAFM), anterolateral MTCAs (SO, MPT, PT, PTTZ, and FTOZ), and lateral MTCAs (ST and STTZ), the surgical corridor corresponds to the total space bounded by the nasal structures or the craniotomy window and the intracranial anatomical structures.

Concerning posterolateral MTCAs (RS, FL, and presigmoid approaches), the surgical corridors were quantified using the routes to the clivus limited by the neurovascular structures of the pontocerebellar angle (PCA) for a total of 10 different surgical corridors (Fig. 2): the sum of these was considered the total working space of the approach. During volume tracking, the vertebral artery was gently displaced and cerebellar retraction was kept constant with brain retractors [11].

Radiological reconstructions of the surgical pyramids (i.e., the working volume) were available in real time in

Fig. 2 Quantified crossing posterolateral MTCAs to the clivus. ▶ Exemplificative screenshots from ApproachViewer (part of GTx-Eyes II – UHN – University of Toronto) in axial, coronal, and sagittal planes and 3-dimensional view of crossing posterolateral microsurgical transcranial approaches. **a** Retrosigmoid approach. **b** Far-lateral approach. **c** Presigmoid retrolabyrinthine infratentorial approach. **d** Presigmoid translabyrinthine infratentorial approach. **e** Presigmoid transcochlear infratentorial approach. 10 surgical pathways of posterolateral MTCAs to the clivus were identified and quantified as follows: (1) between trochlear nerve and trigeminal stem (green—pathway 1); (2, 3) between the trigeminal stem and the acoustic-facial bundle both above (red—pathway 2a) and below (yellow—pathway 2b) the abducens nerve; (4, 5) between the acoustic-facial bundle and the glossopharyngeal nerve both above (light blue—pathway 3a) and below (fuchsia—pathway 3b) the abducens nerve; (6) between the glossopharyngeal and vagus nerves (orange—pathway 4); (7, 8) Between the vagus nerve and the spinal root of the accessory nerve both above (blue—pathway 5a) and below (brown—pathway 5b) the hypoglossal nerve; (9, 10) below the hypoglossal nerve, both anterior (white—pathway 6a) and posterior (gray—pathway 6b) of the spinal root of the accessory nerve

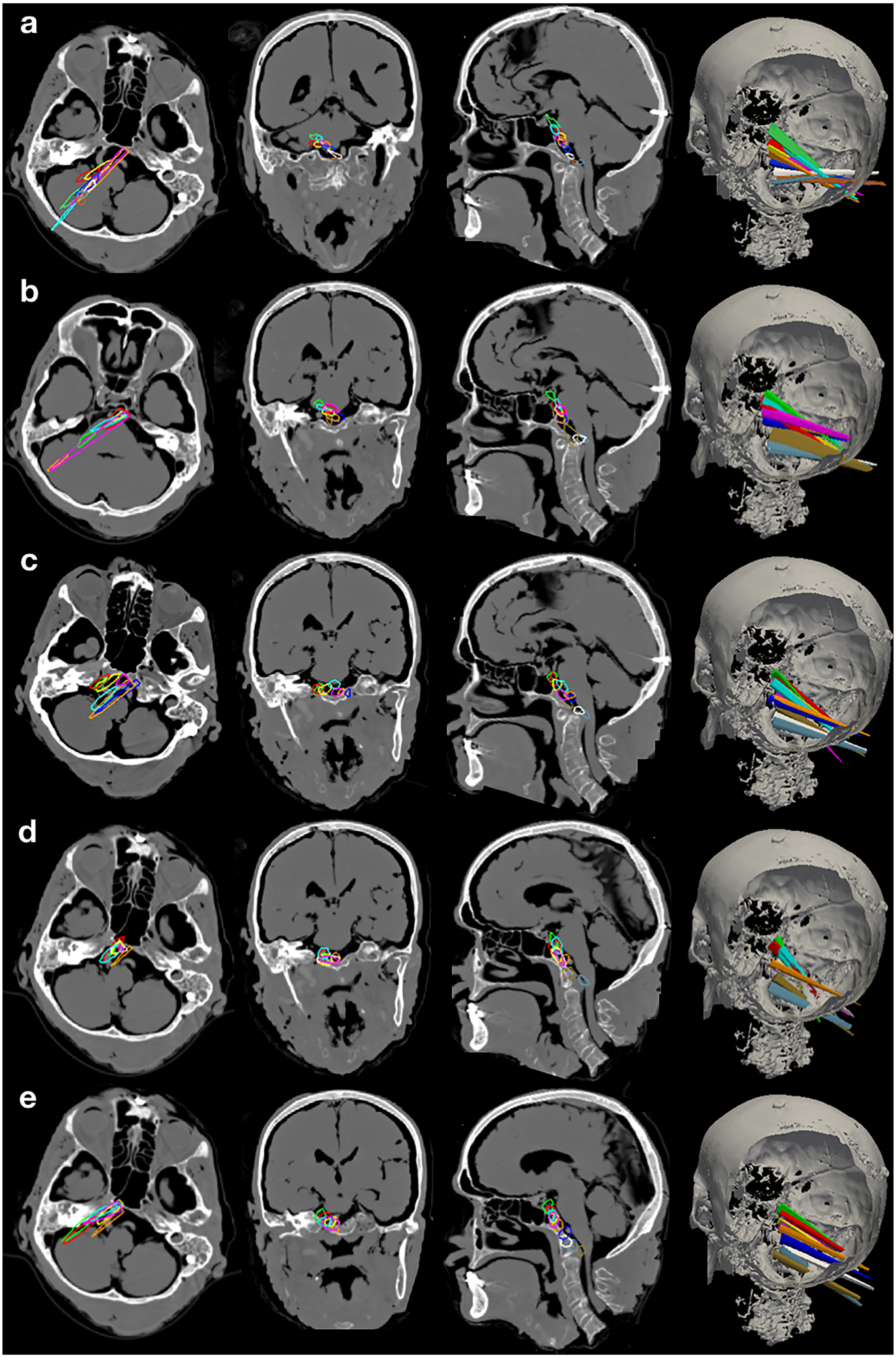
a
b
c
d
e

ApproachViewer, on the coronal, sagittal, and axial CT images, as well as in a 3D view.

Quantification of the surgical corridors was performed in non-crossing and crossing positions, as described by Belotti et al. [3], and repeated three times for each modality.

Thanks to a recent refinement of the software, only the deep surface of the surgical corridor was tracked using a navigation pointer, contouring the perimeter of the reachable portions of the exposed clivus (Qiu et al. 2019, unpublished data). The superficial surface was tracked simultaneously and automatically at a preset height through the "tool length" function of ApproachViewer. For MTCAs, tool length was set at 90 mm, whereas for ETCAs, it was 120 mm. Subsequently, the surgical pyramid was cut at the level of the craniotomy (MCTAs) or nostrils (ECTAs), and ApproachViewer calculated the volume of the surgical pyramid (Qiu et al. 2019, unpublished data).

Surface rendering

ITK-SNAP [46] software was used to render the surfaces of interest on each CT scan. Drawings were performed tracing a line from one side to another of the desired slice on axial, sagittal, and coronal CT images. Subsequently, the software automatically assembled lines to generate the surface.

Sixteen clival surfaces were thus defined (Fig. 3): 8 on the intracranial (posterior) clivus and 8 on the extracranial (anterior) clivus.

Each surface was saved in "MetaImage" file format (.mha) to be uploaded on ApproachViewer and exported in "Surface Mesh" with "STL Mesh file" format file (.stl) [38].

Surface area calculation

"STL Mesh file" format file (.stl) was imported in Autodesk Meshmixer 3.5®, and through "analysis," "conversion mm in cm," and "stability" functions, the absolute value of each surface was obtained.

Area of exposure extrapolation

The ".mha" file of drawn surfaces was imported in ApproachViewer, and the software calculated the absolute value of the deep surface included in each pyramid volume.

Finally, data were collected in Microsoft Excel 16.16.1©: the intersection percentage was calculated by dividing each absolute intersection value obtained in ApproachViewer by the total surface area of the corresponding segmentation image obtained in Autodesk Meshmixer 3.5®.

Statistical analysis

Descriptive statistical analysis was used to summarize the main characteristics of the study sample. Linear mixed models were fit to evaluate the association between surface exposure and each surgical volume with random intercepts for specimens, using STATA® software (StataCorp® LLC, College Station, TX, USA). Bootstrap resampling method was used

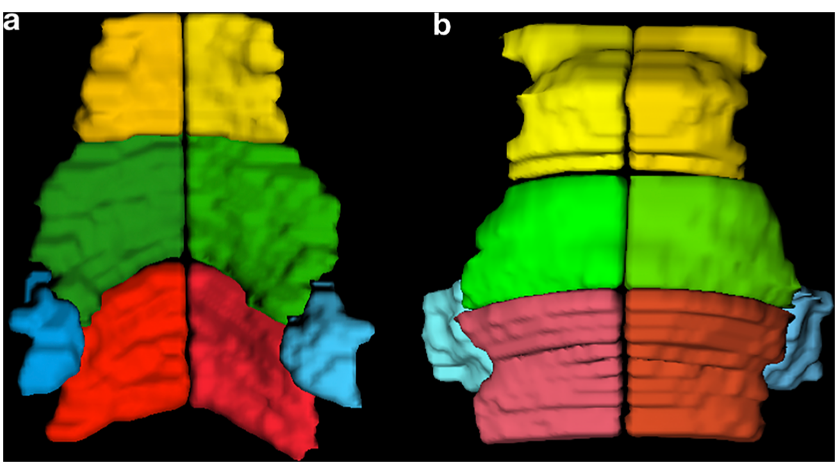

Fig. 3 Anatomical subdivision of the clivus. The 16 surfaces, as drawn on ITK-SNAP, are shown in the posterior, intracranial aspect (**a**) and the anterior, extracranial region (**b**). The upper clivus is depicted in yellow, the middle in green, and the lower in red; the jugular tubercle is colored in blue. Different shades are used for the anterior and posterior surfaces, as well as the left and right sides. The inferior limit of the upper clivus was the axial plane, including the dural entrance of abducens nerves. The inferior limit of the middle clivus was the axial plane, including the dural entrance of glossopharyngeal nerves. The inferior limit of the lower clivus was the axial plane, including the foramen magnum. The lateral margins of the clivus were represented, in a craniocaudal direction, by the ipsilateral posterior clinoid, the lateral portion of the dorsum sellae, the medial limit of the paraclival carotid, and a sagittal plane including the entrance of the hypoglossal nerve in its canal. The medial margin was represented by the midline. The jugular tubercle was drawn in its intracranial portion, and its projection in the axial plane at the level of the cortical clival bone defined its anterior surface

to estimate the 95% confidence interval with 1000-fold replication. Analysis was stratified also for crossing measures. Statistical significance was set at $P < 0.05$.

Results

The mean percentages of the exposed area of each clival surface by each surgical corridor are reported in detail in Supplementary Tables 1–16. The graphical representation of the exposed area of each clival surface offered by each surgical approach is illustrated in Fig. 4.

Statistical analysis of the more than 33,000 collected data showed that ETCAs offer a better clival exposure than MTCAs for all clival surfaces. ETCAFM offers the best exposure of the jugular tubercle with a 46% advantage over ETCA. With ETCAH, an exposure gain of 39% is obtained compared with ETCA. Furthermore, with respect to presigmoid approaches, the greater is the invasiveness of the approach, the better is the exposure of the ipsilateral clivus.

Analyzing the results for every single surface and considering the cranial portion of the clivus, the upper posterior clivus is exposed significantly more by ETCAH compared with ETCAs (Fig. 5a), lateral MTCAs, and posterolateral MTCAs. Among lateral MTCAs, STTZ offers a greater exposure of the upper (anterior and posterior) clivus than ST, but not in a statistically significant way (Supplementary Fig. 3). Regarding the middle and lower posterior clivus, ETCAs offer a significantly wider exposure compared with posterolateral MTCAs; anterolateral and lateral MTCAs do not allow exposure of this region. The posterior jugular tubercle region was exposed significantly more by ETCAFM as compared with other ETCAs (Fig. 5b) and posterolateral MTCAs; anterolateral and lateral MTCAs do not allow exposure of this region.

The upper anterior clivus was exposed more by ETCAH as compared with other ETCAs, anterolateral MTCAs, and lateral MTCAs. Concerning the middle anterior clivus and the lower anterior clivus, all endoscopic transnasal approaches expose the same clival surface. MTCAs do not allow significant exposure to this region. ETCAFM exposes a significantly larger surface of the anterior jugular tubercle region as compared with other ETCAs; MTCAs do not allow exposure of this region.

The mean volume of each surgical approach is reported in Supplementary Table 17 and in Fig. 6. ETCAs had a higher volume than all MTCAs. Among ETCAs, ETCAFM had the greatest working volume. STTZ had a higher working volume than ST. STTZ had a lower working volume than all the

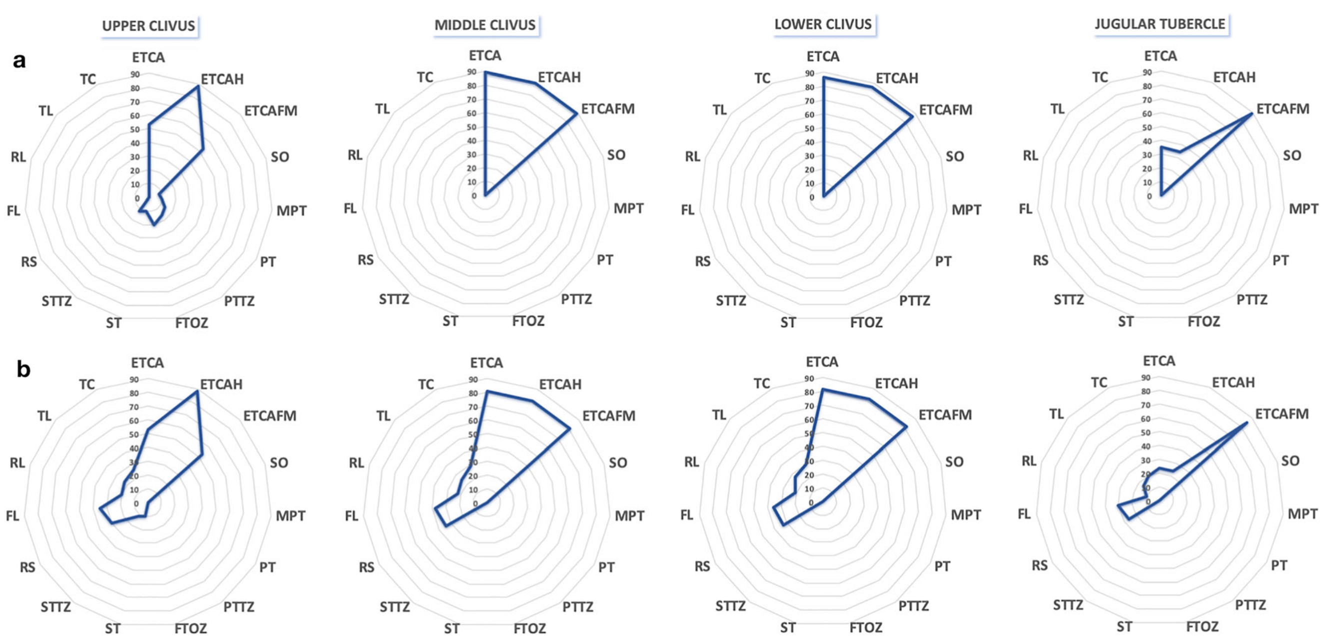

Fig. 4 Exposure of different clival regions by all approaches. The radar diagrams show the percentage value of the exposed area obtained by each approach (as measured in a crossing modality) for the different clival regions. **a** Anterior clival surfaces. **b** Posterior clival surfaces. ETCA, transnasal endoscopic transclival approach; ETCAFM, ETCA with far-medial extension; ETCAH, ETCA with intradural hypophysiopexy; FL, far-lateral approach; FTOZ, fronto-temporal-orbito-zygomatic approach; MPT, mini-pterional approach; PT, pterional approach; PTTZ, pterional transzygomatic approach; RL, presigmoid retrolabyrinthine infratentorial approach; RS, retrosigmoid approach; SO, supraorbital approach; ST, subtemporal approach; STTZ, subtemporal transzygomatic approach; TC, presigmoid transcochlear infratentorial approach; TL, presigmoid translabyrinthine infratentorial approach

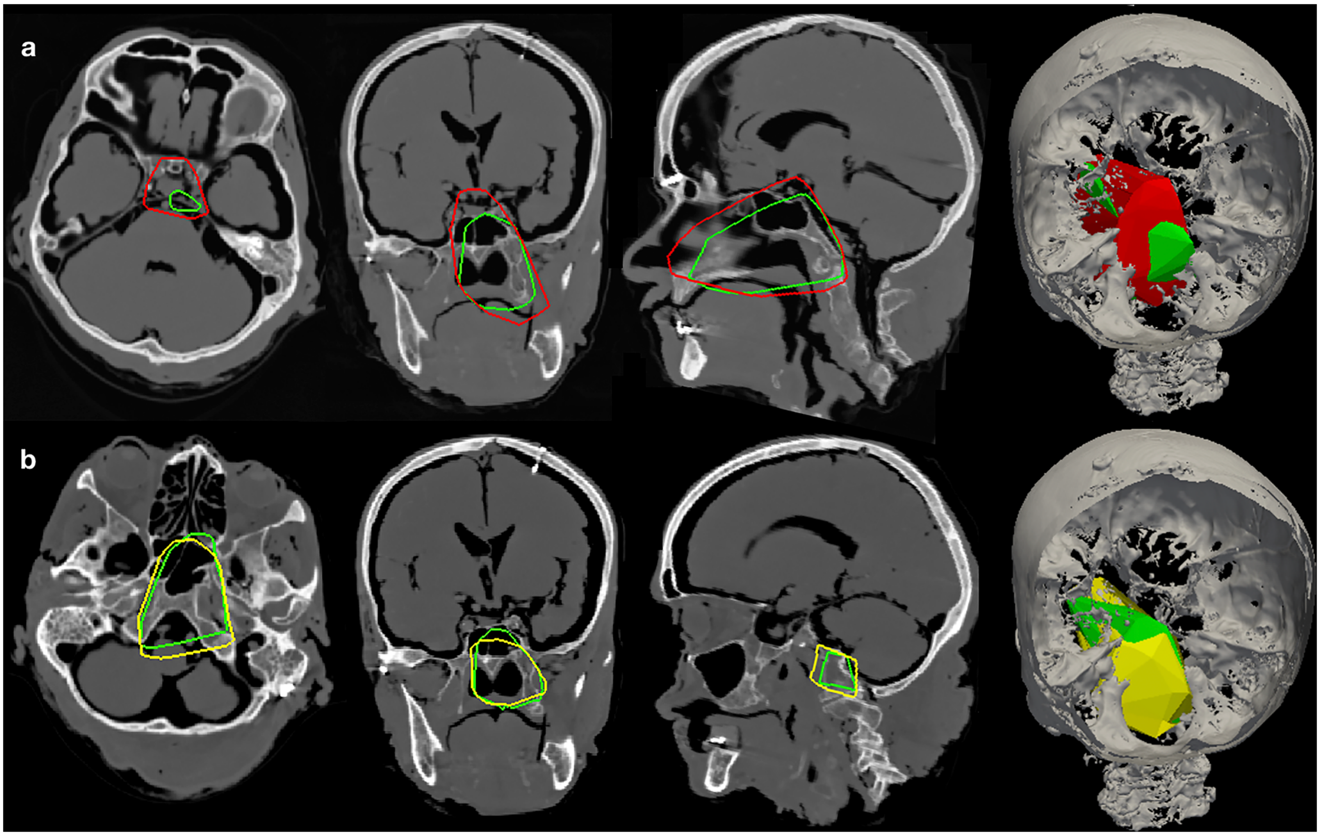

Fig. 5 Comparative analysis of ETCAs. Exemplificative screenshots from ApproachViewer (part of GTx-Eyes II – UHN – University of Toronto) in axial, coronal, and sagittal planes and 3-dimensional view of endoscopic transnasal approaches performed in one specimen and compared. **a** Crossing ETCA (green) and crossing ETCAH (red) are shown, documenting the gain in exposure of the upper (anterior and posterior) clivus offered by the latter approach. **b** Crossing ETCA (green) and crossing ETCAFM (yellow), showing the gain of exposure of the (anterior and posterior) jugular tubercle region obtained by the latter approach. ETCA, transnasal endoscopic transclival approach; ETCAFM, ETCA with far-medial extension; ETCAH, ETCA with intradural hypophysiopexy

posterolateral and anterolateral MTCAs, except for SO. Among anterolateral MTCAs, FTOZ offered the most significant working volume, whereas, among posterolateral MTCAs, FL guaranteed the greatest working volume.

Discussion

Recently, our group published a limited comparative analysis of some approaches to the clivus [11]. With this new study, new data have been produced, and the research method has been improved (Qiu et al. 2019, unpublished data), to create a broader comparison that considers all the most used modern approaches to the clivus.

In this anatomical study, using modern stereotactic computer-based techniques, it was found that ETCAs objectively provide an advantage in terms of clival exposure, when compared with MTCAs. It was also shown that ETCAs guarantee a fair exposure of lateral anatomical structures, significantly exposing the jugular tubercle with ETCAFM. In addition, it has been demonstrated that anterolateral MTCAs are an excellent route to selectively expose the posterior clinoid process. Another expected evidence was the larger exposure of the ipsilateral clivus offered by the presigmoid approaches in proportion to their invasiveness.

This study showed that ETCAs generally offer a greater exposure of all clival portions than MTCAs. The advantage of ETCAs is to offer a direct corridor to the clivus without major neurovascular structures interposed. This is possibly the reason that has led different authors to recently use ETCAs also for the treatment of intradural pathologies [1, 3, 17, 29, 31], although a significant postoperative cerebrospinal fluid (CSF) leak risk still limits the approach in these cases [18, 19, 21, 47].

While it is well established that ETCAs provide better exposure of midline structures, there is still less information about the possible advantages of endoscopic approaches to transcranial approaches in relation to the exposure of lateral structures. Several authors underlined the limited ability of ETCAs to expose lateral structures such as jugular tubercles [8, 27], while other authors already underlined the potential

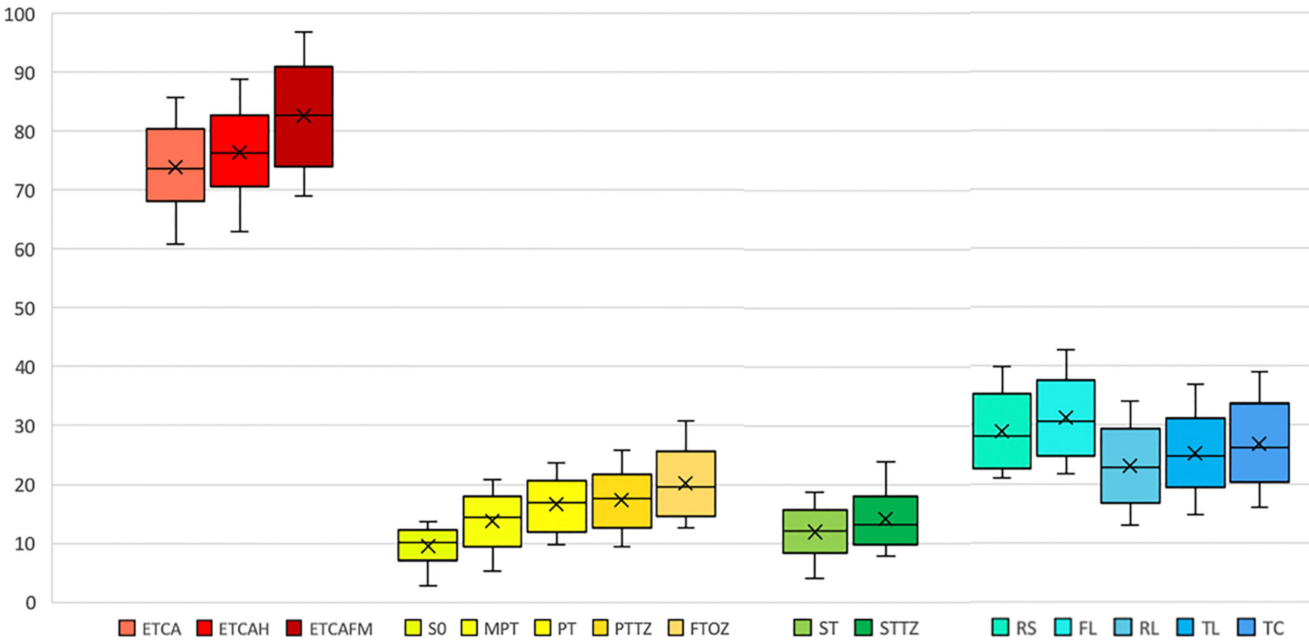

Fig. 6 Analysis of surgical volume provided by the different approaches. Boxplot representation of ETCAs (red) and anterolateral (yellow), lateral (green), and posterolateral (blue) MTCAs. Each boxplot indicates minimum, first quartile, median (middle bar), average (cross), third quartile, and maximum values of each surgical volume. Volumetric values are in cm^3. ETCA, transnasal endoscopic transclival approach; ETCAFM, ETCA with far-medial extension; ETCAH, ETCA with intradural hypophysiopexy; FL, far-lateral approach; FTOZ, fronto-temporal-orbito-zygomatic approach; MPT, mini-pterional approach; PT, pterional approach; PTTZ, pterional transzygomatic approach; RL, presigmoid retrolabyrinthine infratentorial approach; RS, retrosigmoid approach; SO, supraorbital approach; ST, subtemporal approach; STTZ, subtemporal transzygomatic approach; TC, presigmoid transcochlear infratentorial approach; TL, presigmoid translabyrinthine infratentorial approach

for reaching the ventromedial brainstem offered by far-medial approach [11, 32]. Another original finding of the present study is the demonstration of the lateral extension capacity of endoscopic approaches, with a statistically significant gain of exposure of the jugular tubercles offered by ETCAFM with respect to ETCA (Fig. 5b).

The possibility of exposure of the superior clivus, and in particular the posterior clinoid process, has been little described in the literature. For example, Nutik [33] reported a case of removal of a posterior clinoid process meningioma through a pterional approach. The innovative finding of this study was that all anterolateral MTCAs offer a direct route for posterior clinoid process exposure, regardless of the size of the craniotomy. This demonstrated how, for pathologies with localization limited to the anterior face of the posterior clinoid process (such as meningiomas [40]), it is possible to use an anterolateral MTCA with limited invasiveness, such as the SO, to facilitate complete and safe removal of the lesion (Fig. 7).

Furthermore, this study demonstrated the limited ability of exposing the ipsilateral clivus offered by the presigmoid approach, due to the interposition of the petrous bone. Nevertheless, it has been proved that the major was the drilling of the petrous bone and the greater was the exposure of the ipsilateral clivus offered by a presigmoid approach. This explains why the TC offers a larger exposure of the ipsilateral clivus than the other presigmoid approaches, although not in a statistically significant way. Therefore, it is possible to state objectively that the invasiveness of transpetrosal approaches does not justify their employment to gain access to the ipsilateral clivus. RS provides adequate exposure of the ipsilateral clivus while limiting morbidity to the potential injury of PCA neurovascular structures (Supplementary Fig. 4).

Limitations of the study

This is a preclinical study, so it did not consider the possible increase in working volume and anatomical distortion caused by a tumor or other space-occupying lesions nor the position of relevant vascular and neural structures in relation to the mass that has to be treated. Despite the objective data of working volumes and exposure areas obtained with a defined approach, it is important to note that no surgical approach can be recommended over another based on a preclinical study alone.

Although the quantification and comparison of the approaches in the same specimen minimized any potential variability related to different brain characteristics and anatomical variations, further studies are necessary to investigate the

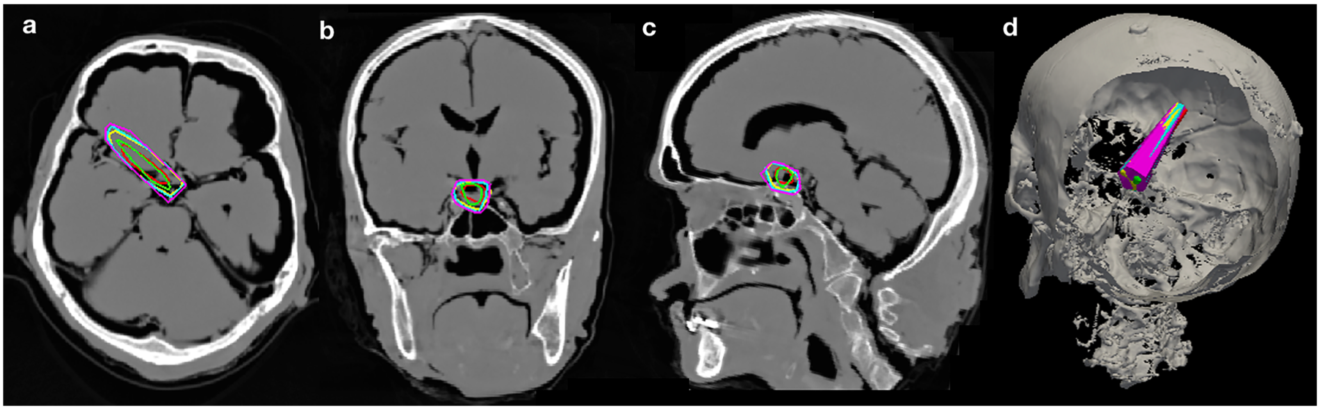

Fig. 7 Comparative analysis of anterolateral MTCAs. Exemplificative screenshots from ApproachViewer (part of GTx-Eyes II – UHN – University of Toronto) in axial, coronal, and sagittal planes and 3-dimensional view of crossing anterolateral microsurgical approaches to the (upper) clivus. Different colors depict different approaches: supraorbital in green, mini-pterional in red, pterional in yellow, pterional-transzygomatic in light blue, and fronto-temporal-orbito-zygomatic in fuchsia

possible influence of anatomical variations on the choice of the surgical approach.

Notably, fixation-induced shrinkage and hardening of the brain and sinonasal structures might have affected the quantification of surgical approaches.

Furthermore, this study is aimed at providing a complete overview of all the most widely used approaches to the clivus. Further anatomical studies may be performed to analyze and compare specific approaches to single clival areas.

Conclusions

This is the first anatomical study that quantitatively compares exposure areas and working volumes provided by the most used approaches to the clivus in modern surgical practice. Although this study is limited to a preclinical evaluation, it is possible to integrate its findings in the more complex clinical scenario, thus tailoring the approach to the single patient.

Acknowledgments We thank Prof. R. Rezzani, Ph.D., Head of the Section of Anatomy and Pathophysiology of Brescia, for study support, Prof. Giuseppe Lanzino, M.D., for study supervision, and Elisa Colombo, M.S., for her guidance.

Compliance with ethical standards

Conflict of interest The authors declare that they have no conflict of interest.

Research involving human participants and/or animals and informed consent This work was performed according to the ethical standards of our Institutional Review Board. All human cadaveric studies have been performed in accordance with the ethical standards laid down in the 1964 Declaration of Helsinki and its later amendments. The manuscript does not contain clinical studies or patient data.

Abbreviations CSF, cerebrospinal fluid; CT, computed tomography; DICOM, Digital Imaging and Communications in Medicine; ETCA, endoscopic transnasal transclival approach; ETCAs, endoscopic transnasal transclival approaches; ETCAFM, ETCA with far-medial extension; ETCAH, ETCA with intradural hypophysiopexy approach; FL, Far-lateral approach; FTOZ, Fronto-temporal-orbito-zygomatic approach; GTx-Eyes II – UHN, Guided Therapeutics software developed at University Health Network – Toronto, Canada; IDEAL, Innovation Development Exploration Assessment Long term; IACs, internal acoustic canals; MPT, mini-pterional approach; MTCAs , microsurgical transcranial approaches; PT, pterional approach; PTTZ, pterional transzygomatic approach; SO, supraorbital approach; RL, presigmoid retrolabyrinthine infratentorial approach; RS, retrosigmoid approach; ST, subtemporal approach; STTZ, subtemporal transzygomatic approach; TC, presigmoid transcochlear infratentorial approach; TL, presigmoid translabyrinthine infratentorial approach

References

1. Beer-Furlan A, Abi-Hachem R, Jamshidi AO, Carrau RL, Prevedello DM (2016) Endoscopic trans-sphenoidal surgery for petroclival and clival meningiomas. J Neurosurg Sci 60:495–502
2. Belotti F, Doglietto F, Schreiber A et al (2018) Modular classification of endoscopic endonasal transsphenoidal approaches to sellar region: anatomic quantitative study. World Neurosurg. 109:281–291
3. Belotti F, Tengattini F, Mattavelli D, Ferrari M, Fiorentino A, Agnelli S, Buffoli B, Schreiber A, Maroldi R, Rodella L, Nicolai P, Fontanella MM, Doglietto F (2019) Transclival approaches for intradural pathology: Historical overview and present scenario. Neurosurgical Review (submitted)
4. Beltrán-Giner A, Miranda-Lloret P, Plaza-Ramirez E, Simal-Julián J-A, Botella-Asunción C (2013) Full endoscopic endonasal extreme far-medial approach: eustachian tube transposition. J Neurosurg Pediatr 11:584–590
5. Campero A, Campero AA, Socolovsky M, Martins C, Yasuda A, Basso A, Rhoton A (2010) The transzygomatic approach. J Clin Neurosci 17:1428–1433
6. Cook JA, McCulloch P, Blazeby JM, Beard DJ, Marinac-Dabic D, Sedrakyan A, IDEAL Group (2013) IDEAL framework for surgical innovation 3: randomised controlled trials in the assessment stage and evaluations in the long term study stage. BMJ. 346:2820
7. Daly MJ, Chan H, Nithiananthan S, Qiu J, Barker E, Bachar G, Dixon BJ, Irish JC, Siewerdsen JH (2011) Clinical implementation

of intraoperative cone-beam CT in head and neck surgery. Proc. SPIE 7964, Medical Imaging 2011: Visualization, Image-Guided Procedures, and Modeling, 796426 (1 March 2011); https://doi.org/10.1117/12.878976
8. De Arnaldo Silva Vellutini E, Balsalobre L, Hermann DR, Stamm AC (2014) The endoscopic endonasal approach for extradural and intradural clivus lesions. World Neurosurg. 82:106–115
9. De Notaris M, Cavallo LM, Prats-Galino A, Esposito I, Benet A, Poblete J, Valente V, Gonzalez JB, Ferrer E, Cappabianca P (2009) Endoscopic endonasal transclival approach and retrosigmoid approach to the clival and petroclival regions. Neurosurgery. 65:42–50
10. Doglietto F, Belotti F, Qiu J et al (2019) Endonasal and transoral approaches to the craniovertebral junction: a quantitative anatomical study. Acta Neurochir Suppl 125:37–44
11. Doglietto F, Ferrari M, Mattavelli D et al (2018) Transnasal endoscopic and lateral approaches to the clivus: a quantitative anatomic study. World Neurosurg 113:659–671
12. Dolenc VV (1994) Frontotemporal epidural approach to trigeminal neurinomas. Acta Neurochir 130:55–65
13. Ergina PL, Barkun JS, McCulloch P, Cook JA, Altman DG, IDEAL Group (2013) IDEAL framework for surgical innovation 2: observational studies in the exploration and assessment stages. BMJ. 346:3011
14. Ferrari M, Schreiber A, Mattavelli D et al (2016) The inferolateral transorbital endoscopic approach: a preclinical anatomic study. World Neurosurg. 90:403–413
15. Ferrari M, Schreiber A, Mattavelli D, Lombardi D, Rampinelli V, Doglietto F, Rodella LF, Nicolai P (2018) Surgical anatomy of the parapharyngeal space: a multiperspective, quantification-based study. Head Neck 41:642–656
16. Figueiredo EG, Deshmukh P, Nakaji P, Crusius MU, Crawford N, Spetzler RF, Preul MC (2007) The minipterional craniotomy: technical description and anatomic assessment. Neurosurgery. 61:256–264
17. Gardner PA, Vaz-Guimaraes F, Jankowitz B, Koutourousiou M, Fernandez-Miranda JC, Wang EW, Snyderman CH (2015) Endoscopic endonasal clipping of intracranial aneurysms: surgical technique and results. World Neurosurg. 84:1380–1393
18. Gruss CL, Al Komser M, Aghi MK, Pletcher SD, Goldberg AN, McDermott M, El-Sayed IH (2014) Risk factors for cerebrospinal leak after endoscopic skull base reconstruction with nasoseptal flap. Otolaryngol Head Neck Surg (United States) 151:516–521
19. Hadad G, Bassagasteguy L, Carrau RL, Mataza JC, Kassam A, Snyderman CH, Mintz A (2006) A novel reconstructive technique after endoscopic expanded endonasal approaches: vascular pedicle nasoseptal flap. Laryngoscope. 116:1882–1886
20. Jägersberg M, Brodard J, Qiu J, Mansouri A, Doglietto F, Gentili F, Kucharczyk W, Fasel J, Schaller K, Radovanovic I (2017) Quantification of working volumes, exposure, and target-specific maneuverability of the pterional craniotomy and its minimally invasive variants. World Neurosurg 101:710–717
21. Kamat A, Lee JYK, Goldstein GH, Newman JG, Storm PB, Palmer JN, Adappa ND (2015) Reconstructive challenges in the extended endoscopic transclival approach. J Laryngol Otol 129:468–472
22. Kassam A, Snyderman CH, Mintz A, Gardner P, Carrau RL (2005) Expanded endonasal approach: the rostrocaudal axis. Part I. Crista galli to the sella turcica. Neurosurg Focus 19:3
23. Kassam A, Snyderman CH, Mintz A, Gardner P, Carrau RL (2008) Expanded endonasal approach: the rostrocaudal axis. Part II. Posterior clinoids to the foramen magnum. Neurosurg Focus 19:4
24. Kassam AB, Gardner P, Snyderman C, Mintz A, Carrau R (2005) Expanded endonasal approach: fully endoscopic, completely transnasal approach to the middle third of the clivus, petrous bone, middle cranial fossa, and infratemporal fossa. Neurosurg Focus 19:6
25. Kassam AB, Prevedello DM, Carrau RRL et al (2011) Endoscopic endonasal skull base surgery: analysis of complications in the authors' initial 800 patients. J Neurosurg 144:1544–1568
26. Kassam AB, Prevedello DM, Thomas A, Gardner P, Mintz A, Snyderman C, Carrau R (2008) Endoscopic endonasal pituitary transposition for a transdorsum sellae approach to the interpeduncular cistern. Neurosurgery. 62:57–72
27. Kim YH, Jeon C, Se Y-B et al (2017) Clinical outcomes of an endoscopic transclival and transpetrosal approach for primary skull base malignancies involving the clivus. J Neurosurg 128:1454–1462
28. Koutourousiou M, Fernandez-Miranda JC, Vaz-Guimaraes Filho F, de Almeida JR, Wang EW, Snyderman CH, Gardner PA (2017) Outcomes of Endonasal and lateral approaches to Petroclival Meningiomas. World Neurosurg. 99:500–517
29. Mangussi-Gomes J, Beer-Furlan A, Balsalobre L, Vellutini EAS, Stamm AC (2016) Endoscopic endonasal management of skull base chordomas: surgical technique, nuances, and pitfalls. Otolaryngol Clin N Am 49:167–182
30. McCulloch P, Altman DG, Campbell WB, Flum DR, Glasziou P, Marshall JC, Nicholl J (2009) No surgical innovation without evaluation: the IDEAL recommendations. Lancet. 374:1105–1112
31. Mesquita Filho PM, Ditzel Filho LFS, Prevedello DM, Martinez CAN, Fiore ME, Dolci RLL, Otto BA, Carrau RL (2014) Endoscopic endonasal surgical management of chondrosarcomas with cerebellopontine angle extension. Neurosurg Focus 37:13
32. Morera VA, Fernandez-Miranda JC, Prevedello DM, Madhok R, Barges-Coll J, Gardner P, Carrau R, Snyderman CH, Rhoton AL, Kassam AB (2010) "Far-medial" expanded endonasal approach to the inferior third of the clivus: the transcondylar and transjugular tubercle approaches. Neurosurgery. 66:211–220
33. Nutik SL (1998) Pterional craniotomy via a transcavernous approach for the treatment of low-lying distal basilar artery aneurysms. J Neurosurg 89:921–926
34. Perneczky A (1999) Key-hole concept in neurosurgery. Springer-Verlag, Vienna, pp 37–95
35. Qiu J, Radovanovic I, Gentili F, Ravichandiran M, Doglietto F, Fontanella MM, Zadeh G, Kucharczyk W, Belotti F, Agur A (2017) Quantitative comparison of cranial approaches in the anatomy laboratory: a neuronavigation based research method. World J Methodol 7:139–147
36. Rhoton J (2000) The far-lateral approach and its transcondylar, supracondylar, and paracondylar extensions. Neurosurgery. 47:195–209
37. Samii M, Knosp E (1992) Approaches to the clivus. Approaches to no man's land. Springer-Verlag, Berlin Heidelberg, pp 1–6
38. Schmidt R, Singh K (2010) Meshmixer: an interface for rapid mesh composition. ACM SIGGRAPH. https://doi.org/10.1145/1837026.1837034
39. Schreiber A, Ferrari M, Rampinelli V, Doglietto F, Belotti F, Lancini D, Ravanelli M, Rodella LF, Fontanella MM, Nicolai P (2017) Modular endoscopic medial maxillectomies: quantitative analysis of surgical exposure in a preclinical setting. World Neurosurg. 100:44–55
40. Sodhi HBS, Singla N, Gupta SK (2015) Posterior clinoid meningioma: a case report with discussion on terminology and surgical approach. Surg Neurol Int 6:21
41. Ustun ME, Buyukmumcu M, Ulku CH, Guney Ö, Salbacak A (2006) Transzygomatic-subtemporal approach for middle meningeal-to-P2 segment of the posterior cerebral artery bypass: an anatomical and technical study. Skull Base 16:39–44
42. Van Furth WR, Agur AMR, Woolridge N, Cusimano MD (2006) The orbitozygomatic approach. Neurosurgery. 58:103–107
43. Vender JR (2013) Retrosigmoid approach. Oper Tech Otolaryngol Head Neck Surg 45:375–397

44. Wanibuchi M, Friedman AH, Fukushima T (2009) Photo atlas of skull base dissections. Thieme, Stuttgart, pp 268–288
45. Yasargil MG (1984) Microneurosurgery, vol 1. Thieme-Stratton, New York, pp 215–233
46. Yushkevich PA, Piven J, Hazlett HC, Smith RG, Ho S, Gee JC, Gerig G (2006) User-guided 3D active contour segmentation of anatomical structures: significantly improved efficiency and reliability. Neuroimage. 31:1116–1128
47. Zwagerman NT, Wang EW, Shin SS, Chang YF, Fernandez-Miranda JC, Snyderman CH, Gardner PA (2018) Does lumbar drainage reduce postoperative cerebrospinal fluid leak after endoscopic endonasal skull base surgery? A prospective, randomized controlled trial. J Neurosurg 1:1–7